Influence of Dufour and Soret on Unsteady, Magneto-hydrodynamics (MHD), Convective Heat and Mass Transfer Flow in Non-Darcy Porous Medium

Gbadeyan, J. A.[1*], Asiru, T. M.[2] and Isede, H. A.[3]

1*, Department of Mathematics, Faculty of Physical Sciences, University of Ilorin, Ilorin, Kwara State.
2, Department of Mathematics, Emmanuel Alayande College of Education, Oyo, Oyo State.
3, Department of Mathematics, University of Lagos, Akoka, Lagos State.
Corresponding Author's email: hisede@unilag.edu.ng

Abstract

This study investigates the influence of Dufour, Soret, radiation and dissipation on an unsteady, free convective heat and mass transfer of a viscous incompressible, gray, absorbing-emitting magnetohydrodynamics (MHD) fluid flowing past an impusively started vertical plate in a porous medium. The governing equations are reduced to two-dimensional and two dependent problems involving velocity, temperature, and concentration with appropriate boundary conditions. The Rosseland diffusion approximation was employed to analyze the radiative heat flux which is appropriate for non-scattering media. The governing equations for the model are simplified and non-dimensionalized. The dimensionless governing equations are solved using an implicit finite-difference method of Crank-Nicolson type. A parametric study is performed to illustrate the influence of the emerging thermophysical parameters (Prandtl number, thermal Grashof number, species Grashof number, etc.) on the velocity, temperature, and concentration profiles. Also, the behaviour of the local and average skin-friction, Nusselt number and Sherwood number are presented graphically. The results obtained are compared with previously published ones and are found to be in excellent agreement. This model finds applications in transport of fires in porous media (forest fires), the design of high temperature chemical processing systems, solar energy collection systems and porous combustors.

1 Introduction

The influence of Dufour, Soret, radiation and dissipation on an unsteady, free convective heat and mass transfer of a viscous incompressible, gray, absorbing-emitting hydromagnetic fluid flowing past an impusively started vertical plate in a porous medium was investigated.

Heat and mass transfer occur simultaneously in many processes such as drying evaporation at the surface of a wet body, energy transfer in a wet cooling tower, flow in a desert cooler, polymer production and food processing. Hence, it is of interest to examine the combined effects of heat and mass transfer with chemical reaction, MHD, Dufour and Soret because of their applications. Loganatha et al. [1], studied the effect of chemical reaction on an unsteady two dimensional free convective heat and mass transfer, past a vertical plate with variable viscosity and thermal conductivity.

Many high temperature processes in the industrial design and combustion and fire science involve thermal radiation, heat transfer in combination with conduction, convection and mass transfer. For example, radiative heat transfer flows arise in industrial furnace systems, astrophysical flows, forest fire dynamics and fire spread in building, Alam et al. [2], Mahjan and Gebhart, [3], Mansour, [4], Modest [5]. Considerable research has therefore been carried out on radiative convective flows in a variety of geometrical configurations using various mathematical models. Bratis and Novotny [6] studied the effects of the thermal radiation on the convection boundary layer-regime of an enclosure. Chang and Kang [7] used a radiative flux diffusion approximation to model the interaction of convective and radiative heat transfer in a two dimensional channel. Hossain et al. [8] studied the effects of thermal radiation and heat transfer on combined forced and free convection boundary layer past a horizontal cylinder. Chamkha et al. [9] discussed the natural convective power-law fluid past a vertical plate embedded in a non-Darcian porous medium in the presence of a homogeneous chemical reaction.

Extensive research work has been published on an impulsively started vertical plate with different boundary conditions. Hall [10] solved the problem of Stewartson by finite difference method of a mixed explicit type which is convergent and stable. Soundalgelar et al. [11] obtained the exact solution of Stokes problem for the case of an infinite vertical plate. For the first time, Muthuenmaraswamy [12] studied the natural convection of the flow past an impulsively started vertical plate with variable surface heat flux. Temperature distribution in the fabric layers were shown to be strongly affected by moisture contents and thermal radiation flux. Generally, for low velocity hydromechanics of porous media, a Dacian model is used which relates the bulk matrix impedance in the regime to the pressure drop. This approach is generally accurate for situations where Reynold number is less than approximately 10. Beyond this value, inertial effects become significant and must be incorporated in mathematical models. Both Darcian and Darcy-Forchheimer (inertial) model have been employed extensively in radiative convection flow in porous media. Chamkha [13] examined the influence of solar radiation on free convection flow in an isotropic, homogeneous porous medium using a computational method. Mohammadein et al. [14] employed a regular two-parameter perturbation analysis while studying radiative flux effects on free convection in a non-Darcian porous medium. They discussed four different flow regimes i.e. flow that is adjacent to the isothermal surface, flow with a uniform heat flux, plane plume flow and also the flow generated from a horizontal line energy source on a vertical adiabatic surface.

Takhar et al. [15] carried out a computational analysis of coupled convection radiation dissipation non-gray gas flow in a non-Darcy porous medium using the Keller-Box implicit scheme. Chamkha et al. [16] investigated the influence of thermal radiation on steady natural convection in a viscoelastic fluid saturated by non-Darcian porous medium using Keller-Box numerical scheme.

Dada and Adefolaju [17] studied dissipation, MHD and Radiation effects on an unsteady convective heat and mass transfer in a Darcy-Forcheimmer porous medium and found out that temperatures increases slightly with the increasing value of magnetic field parameter. This also holds for species concentration. Zueco [18] used network simulation method (NSM) to study the effects of viscous dissipation and radiation on unsteady MHD free convection flow past vertical porous plate.

It is also well known (Idowu et al. [19]) that the effect of viscous dissipation which is often neglected in the studies of laminar convection, can be relevant and important if highly viscous fluids with low thermal conductivity are considered. Viscous dissipation effect in duct flow of molten polymers was examined by Berardi et al. [20].

All the above studies did not consider the combined influence of Dufour, Soret, radiation and dissipation on an unsteady free, convective heat and mass transfer of a viscous incompressible, gray, absorbing-emitting hydromagnetic fluid flowing past an impusively started vertical plate in a non-Darcy porous medium, which this study investigates. The governing boundary value problem is nondimensionalized. The resulting dimensionless problem is found to be characterized by the following thermophysical parameters; thermal Grashof number, species Grashof number, Darcy number, Reynold number, Forchheimer number, magnetic field, Eckert number, Prandtl number, Schmidt number, Dufour number and Soret number. The influence of these parameters on the velocity profile, temperature function and mass transfer function are presented and discussed.

2 Formulation of the Problem

The problem under investigation is made up of an unsteady two-dimensional natural convective laminar flow of a viscous incompressible, electrically conducting, radiating and dissipative fluid past an impulsively started semi-infinite vertical plate under a transverse magnetic field. It is assumed that the fluid is absorbing-emitting, gray and not scattering.

The origin of x'-axis is taken to be at the leading edge of the plate while the gravitational acceleration "g" is assumed acting downward. On the other hand, the y'-axis is taken perpendicular to the plate at the leading edge but the x'-axis is chosen along the plate in the upward direction. At time $t' = 0$, it is assumed that the plate and the fluid are at the ambient temperature T'_∞ and the species concentration C'_∞. On the other hand, for $t' > 0$, the temperature of the plate and the species concentration are denoted by T'_w, (such that $T'_\infty < T'_w$) and C'_w (such that $C'_\infty < C'_w$), respectively.

The corresponding configuration of the system is as shown in Figure 1 below.

At time $t = 0$, the plate commences an impulsive motion in the x'-direction, with constant velocity u_0, and the plate temperature and concentration levels are instantaneously increased and are kept constant thereafter.

Effect of viscous dissipation is considered in the binary mixture and assumed to be very small compared with other chemical species, which are present. A uniformly transverse magnetic field is applied in the direction of flow. The fluid properties are assumed to be constant except for the body forces terms in the momentum equation which are approximated by Boussinesq relations. Thermal radiation is assumed to be present in the form of an uni-directional flux in the y'-direction i.e. q_r is transversed to the vertical surface. Then based on the above assumptions, the governing boundary layer equations with Boussinesq approximation are:

Mass conservation:
$$\frac{\partial u'}{\partial x'} + \frac{\partial v'}{\partial y'} = 0 \tag{1}$$

Momentum conservation:
$$\frac{\partial u'}{\partial t'} + u'\frac{\partial u'}{\partial x'} + v'\frac{\partial u'}{\partial y'} = \nu\frac{\partial^2 u'}{\partial y'^2} + g\beta(T' - T'_\infty) + g\beta^*(C' - C'_\infty) - \frac{\sigma}{\rho}B_0^2 u' - \frac{v}{k}u' - \frac{b}{k}u'^2 \tag{2}$$

Energy equation:
$$\frac{\partial T'}{\partial t'} + u'\frac{\partial T'}{\partial x'} + v'\frac{\partial T'}{\partial y'} = \alpha\frac{\partial^2 T'}{\partial y'^2} + \frac{\nu}{C_p}\left[\frac{\partial u'}{\partial y'}\right]^2 - \frac{1}{\rho C_p}\frac{\partial q_r}{\partial y'} + \frac{D_m K_T}{\rho C_p}\frac{\partial^2 C'}{\partial x'^2} \tag{3}$$

Species conservation:
$$\frac{\partial C'}{\partial t'} + u'\frac{\partial C'}{\partial x'} + v'\frac{\partial C'}{\partial y'} = D\left[\frac{\partial^2 C'}{\partial y'^2}\right] + \frac{D_m K_T}{\rho C_p}\frac{\partial^2 T'}{\partial y'^2} \tag{4}$$

Figure 1: Configuration of the System

The corresponding initial and boundary conditions for the study are prescribed as follows:

$$
\left.
\begin{aligned}
t' = 0, \quad & u' = 0,\ v' = 0,\ T' = T'_\infty, && C' = C'_\infty \\[4pt]
t' > 0, \quad & u' = u_0,\ v' = 0,\ T' = T'_w,\ C' = C'_w && \text{at } y' = 0 \\[4pt]
& u' = 0,\ T' = T'_\infty,\ C' = C'_\infty && \text{at } x' = 0 \\[4pt]
& u' \to 0,\ T' \to T'_\infty,\ C' \to C'_\infty && \text{as } y' \to \infty
\end{aligned}
\right\}
\tag{5}
$$

In equations (1)-(5), u', v' are velocity components in x', y' directions respectively, t' is the time, g is the acceleration due to gravity, β is the volumetric coefficient of thermal expansion, β^* is the volumetric coefficient of expansion with concentration, T' is the temperature of the fluid in the boundary layer, C' is the species concentration in the boundary layer, T'_w is the wall temperature, T'_∞ is the free stream temperature far away from the plate, C'_w is the concentration at the plate, C'_∞ is the free stream concentration in the fluid far away from the plate, k is the permeability of the porous medium, B_0 is the magnetic induction, ν is the kinematic viscosity, α is the fluid thermal diffusivity, ρ is the density of the fluid, C_p is the specific heat constant pressure, q_r is the radiation heat flux, D is the species diffusivity, D_m is the species diffusion coefficient, σ is the electrical conductivity of the fluid and K_T is the thermal diffusion ratio.

By the Rosseland approximation (Brewster [21]), the radiative heat flux q_r is given by

$$
q_r = -\frac{4\sigma_s}{3k_e}\frac{\partial T'^4}{\partial y'}
\tag{6}
$$

where σ_s is the Stefan-Boltzmann constant and k_e is the mean absorption coefficient. It should be noted that by using the Rosseland approximation the present analysis is limited to optically thick fluids. If temperature differences within the flow are sufficiently small, then equation (6) can be linearized by expanding T'^4 into the Taylor series about T'_∞, which after neglecting higher order terms takes the form

$$T'^4 \cong 4T'^3_\infty T' - 3T'^4_\infty \tag{7}$$

In view of equations (6) and (7), equation (3) reduces to:

$$\frac{\partial T'}{\partial t'} + u'\frac{\partial T'}{\partial x'} + v'\frac{\partial T'}{\partial y'} = \alpha\frac{\partial^2 T'}{\partial y'^2} + \frac{\nu}{C_p}\left[\frac{\partial u'}{\partial y'}\right]^2 + \frac{16\sigma_s T'^3_\infty}{3k_e\rho C_p}\frac{\partial^2 T'}{\partial y'^2} + \frac{D_m K_T}{\rho C_p}\frac{\partial^2 c'}{\partial x'^2} \tag{8}$$

Equations (1), (2), (4) and (8) with boundary conditions in equation (5) constitute a two-point boundary value problem which is fairly challenging to solve. Next we non-dimensionalize the model by introducing the following non-dimensional quantities:

$$\left.\begin{aligned}
&X = \frac{x'u_0}{v},\ Y = \frac{y'u_0}{v},\ U = \frac{u'}{u_0},\ V = \frac{v'}{u_0},\ E_c = \frac{u_0^2}{C_p(T'_w - T'_\infty)} \\[2mm]
&t = \frac{t'u_0^2}{v},\ T = \frac{T' - T'_\infty}{T'_w - T'_\infty},\ C = \frac{C' - C'_\infty}{C'_w - C'_\infty},\ R = \frac{u_0 L}{v} \\[2mm]
&Pr = \frac{v}{\alpha},\ Sc = \frac{v}{D},\ Da = \frac{k}{L^2},\ Fs = \frac{b}{L},\ N = \frac{k_e k}{4\sigma_s T'^3_\infty},\ M = \frac{\sigma B_0^2 v}{\rho u_0'^2} \\[2mm]
&Gr = \frac{g\beta\nu(T'_w - T'_\infty)}{u_0^3},\ Gm = \frac{g\beta^*\nu(C'_w - C'_\infty)}{u_0^3},\ Sr = \frac{D_m K_T(T'_w - T'_\infty)}{\rho v C_p(C'_w - C'_\infty)}, \\[2mm]
&Du = \frac{D_m K_T(C'_w - C'_\infty)}{\rho C_p v(T'_w - T'_\infty)}
\end{aligned}\right\} \tag{9}$$

where X and Y are dimensionless coordinates, U and V are dimensionless velocities, t is the dimensionless time, T is the dimensionless temperature function, C is the dimensionless concentration function, ν is the conduction radiation heat transfer parameter, Pr is the Prandtl number, Sc is the Schimdt number, Da is the Darcy number, Fs is the Forchheimer (non-Darcy) initial number, Re is the Reynold number, Gr is the thermal Grashof number, Gm is the species Grashof number, M is the magnetic field parameter, Ec is the Eckert number, Sr is the Soret number and Du is the Dufour number.

Applying these non-dimensional quantities in equation (9), the set of equations (1), (2), (4) and (8) reduces to the following non-dimensional equations

$$\frac{\partial U}{\partial X} + \frac{\partial V}{\partial Y} = 0 \tag{10}$$

$$\frac{\partial U}{\partial t} + U\frac{\partial U}{\partial X} + V\frac{\partial U}{\partial Y} = G_r T + G_m C + \frac{\partial^2 U}{\partial Y^2} - MU - \frac{U}{Re^2 Da} - \frac{F_s U^2}{DaRe} \tag{11}$$

$$\frac{\partial T}{\partial t} + U\frac{\partial T}{\partial X} + V\frac{\partial T}{\partial Y} = \frac{1}{Pr}\left[1 + \frac{4}{3N}\right]\frac{\partial^2 T}{\partial Y^2} + Ec\left[\frac{\partial U}{\partial Y}\right]^2 + Du\frac{\partial^2 C}{\partial X^2} \tag{12}$$

$$\frac{\partial C}{\partial t} + U\frac{\partial C}{\partial X} + V\frac{\partial C}{\partial Y} = \frac{1}{Sc}\frac{\partial^2 C}{\partial Y^2} + Sr\frac{\partial^2 T}{\partial Y^2} \tag{13}$$

The corresponding initial and boundary conditions take the form

$$
\left.
\begin{array}{llll}
t \leq 0, & U = 0, & V = 0, & T = 0, \quad C = 0 \\[2mm]
t > 0, & U = 1, & V = 0, & T = 1, \quad C = 1 \quad \text{at } Y = 0 \\[2mm]
& U = 0, & & T = 0, \quad C = 0, \quad \text{at } X = 0 \\[2mm]
& U \to 0, & & T \to 0, \quad C \to 0 \quad \text{at } Y \to \infty
\end{array}
\right\}
\tag{14}
$$

For the type of fluid under consideration, the local as well as average values of skin-friction, Nusselt number and Sherwood number are important, and these are given in dimensionless form as reported by Modest [5] as follows:

$$
\tau_X = \left[\frac{\partial U}{\partial Y} \right]_{Y=0}, \quad \bar{\tau} = -\int_0^1 \left[\frac{\partial U}{\partial Y} \right]_{Y=0} dX
\tag{15}
$$

$$
Nu_x = -X \left[\frac{\partial T}{\partial Y} \right]_{Y=0}, \quad \overline{NU} = -\int_0^1 \left[\frac{\partial T}{\partial Y} \right]_{Y=0} dX
\tag{16}
$$

$$
Sh_X = -X \left[\frac{\partial C}{\partial Y} \right]_{Y=0}, \quad \overline{Sh} = \int_0^1 \left[\frac{\partial C}{\partial Y} \right]_{Y=0} dX
\tag{17}
$$

3   Method of Solution

The coupled nonlinear partial differential equations (10), (11), (12) and (13) with boundary conditions (14) are solved using an implicit finite difference method of Crank-Nicolson type. Following Suneetha and Bhaskar [22]) we consider a rectangular region with X varying from 0 to 1 and Y varying from 0 to $Y_{\max} = 14$ where $Y_{\max}$ corresponds to $Y = \infty$ and $X = 1$ corresponds to the height of the plate. The co-ordinate (X, Y, t) of the mesh points of the solution is defined by $X = i \triangle X, Y = j \triangle Y$, and $t = k \triangle t$, where i, j are positive integers and k is a non negative integer. The values of U at these mesh points are denoted by $U(i \triangle X, j \triangle Y, k \triangle t) = U_{ij}^k$. The finite difference equations corresponding to equations (10), (11), (12) and (13) are given as follows

$$
\left.
\begin{array}{l}
\dfrac{[U_{i,j}^{k+1} - U_{i-1,j}^{k+1} + U_{i,j}^k - U_{i-1,j}^k + U_{i,j-1}^{k+1} - U_{i-1,j-1}^{k+1} + U_{i,j-1}^k - U_{i-1.j-1}^k]}{4 \triangle X} \\[4mm]
+ \dfrac{[V_{i,j}^{k+1} - V_{i,j-1}^{k+1} + V_{i,j}^k - V_{i,j-1}^k]}{2 \triangle Y} = 0
\end{array}
\right\}
\tag{18}
$$

$$
\begin{aligned}
& \left[\frac{U_{ij}^{k+1} - U_{ij}^k}{\triangle t} \right] + \frac{U_{ij}^k \left[U_{i,j}^{k+1} - U_{i-1,j}^{k+1} + U_{i,j}^k - U_{i-1,j}^k \right]}{2 \triangle X} \\[3mm]
& + \frac{V_{ij}^k \left[U_{i,j+1}^{k+1} - U_{ij-1}^{k+1} + U_{ij+1}^k - U_{i,j-1}^k \right]}{4 \triangle Y} \\[3mm]
= \; & \frac{Gr \left[T_{i,j}^{k+1} + T_{i,j}^k \right]}{2} + \frac{Gm \left[C_{i,j}^{k+1} + C_{i,j}^k \right]}{2} \\[3mm]
& + \frac{\left[U_{i,j-1}^{k+1} - 2U_{i,j}^{k+1} + U_{i,j+1}^{k+1} + U_{i,j+1}^k - 2U_{i,j}^k + U_{ij-1}^k \right]}{2(\triangle Y)^2} \\[3mm]
& - \frac{1}{DaRe^2} \frac{\left[U_{i,j}^{k+1} + U_{i,j}^k \right]}{2} - \frac{F_s}{DaRe} \frac{U_{i,j}^k [U_{i,j}^{k+1} + U_{i,j}^k]}{2} - \frac{M [U_{i,j}^{k+1} + U_{i,j}^k]}{2}
\end{aligned}
\tag{19}
$$

$$
\left[\frac{T_{i,j}^{k+1} - T_{i,j}^{k}}{\triangle t}\right] + \frac{U_{i,j}^{k}\left[T_{i,j}^{k+1} - T_{i-1,j}^{k+1} + T_{i,j}^{k} - T_{i-1,j}^{k}\right]}{2\triangle X}
$$

$$
+ \frac{V_{i,j}^{k}\left[T_{i,j+1}^{k+1} - T_{i,j-1}^{k+1} + T_{i,j+1}^{k} - T_{i,j-1}^{k}\right]}{4(\triangle Y)}
$$

$$
= \frac{1}{Pr}\left[1 + \frac{4}{3N}\right]\frac{\left[T_{i,j-1}^{k+1} - 2T_{i,j}^{k+1} + T_{i,j+1}^{k+1} + T_{i,j-1}^{k} - 2T_{i,j}^{k} + T_{i,j+1}^{k}\right]}{2(\triangle Y)^2}
$$

$$
+ Ec\left[\frac{U_{i,j+1}^{k} - U_{i,j}^{k}}{\triangle Y}\right]^2 + \frac{Du\left[C_{i+1,j}^{k+1} - 2C_{i,j}^{k+1} + C_{i-1,j}^{k+1} + C_{i+1,j}^{k} - 2C_{i,j}^{k} + C_{i-1,j}^{k}\right]}{2(\triangle X)^2} \qquad (20)
$$

$$
\frac{C_{i,j}^{k+1} - C_{i,j}^{k}}{\triangle t} + \frac{U_{i,j}^{k}\left[C_{i,j}^{k+1} - C_{i-1,j}^{k+1} + C_{i,j}^{k} - C_{i-1,j}^{k}\right]}{2(\triangle X)}
$$

$$
+ \frac{V_{i,j}^{k}\left[C_{i,j+1}^{k+1} - C_{i,j-1}^{k+1} + C_{i,j+1}^{k} - C_{i,j-1}^{k}\right]}{4\triangle Y}
$$

$$
= \frac{1}{Sc}\frac{\left[C_{i,j-1}^{k+1} - 2C_{i,j}^{k+1} + C_{i,j+1}^{k+1} + C_{i,j-1}^{k} - 2C_{i,j}^{k} + C_{i,j+1}^{k}\right]}{2(\triangle Y)^2}
$$

$$
+ \frac{Sr\left[T_{i,j+1}^{k+1} - 2T_{i,j}^{k+1} + T_{i,j-1}^{k+1} + T_{i,j+1}^{k} - 2T_{i,j}^{k} + T_{i,j-1}^{k}\right]}{2(\triangle Y)^2} \qquad (21)
$$

The subscript i implies the grid point along the X-direction, j along the Y-direction and k along t-direction. We therefore divide X and Y into M and N grid spacing respectively. The mesh sizes are $\triangle X = 0.1$, $\triangle Y = 0.25$ and $\triangle t = 0.01$.

In the computations, as discussed in Suneetha and Bhaskar [22] and Dada and Adefolaju [17], the coefficient $U_{i,j}^{k}$ and $V_{i,j}^{k}$ appearing in the difference equations are treated as constants in any one time step. The values of C, T, U and V are known at all grid point at $t = 0$ from the initial conditions. The value of C, T, U and V at $(k+1)^{th}$ time level are calculated using the known values at previous time level (k). The finite difference equation (21) at every nodal point on a particular i-level constitutes a tridiagonal system of equations, which is solved by the aid of Matlab package using Thomas algorithm as discussed in Carnahan, Luther and Willkes [23]. Hence the values of C are known at every internal nodal point on a particular i at $(k + 1)^{th}$ time level. Similarly, the value of T are calculated from equation (20). Using the value of C and T at $(k + 1)^{th}$ time level in equation (19), the values of U at $(k + 1)^{th}$ time level are found in a similar manner. Then the values of V are calculated explicitly using equation (18) at every nodal point at particular i-level at $(k + 1)^{th}$ time level. This process is repeated for various i-levels. Thus the values of C, T, U and V are known, at all grid points in the rectangular region at $(k + 1)^{th}$ time level. The process is repeated several times for various i-level until the required time is reached. To test the accuracy of the results, we have compared the velocity profile against Y for various thermal Grashof number, Species Grashof number, Schmit number and Conduction-radiation parameter with the Crank-Nicolson computation of Ramachandra Prasad et al. [24]) by setting the values $M = 0$, $Da \to \infty$ $(Da = 10^9)$ and $F_s = 0$ in our finite difference equations and the mesh sizes are taken to be $\triangle X = 0.05$, $\triangle Y = 0.25$ and $\triangle t = 0.01$. The local truncation error is $O(\triangle t^2 + \triangle y^2 + \triangle x)$ and it tends to zero as $\triangle t$, $\triangle x$, and $\triangle y$ respectively tends to zero. Thus the scheme is compatible. According to Ramachandra Prasad et al. [25], the finite difference scheme is unconditionally stable. Hence compatibility and stability ensures the convergence of the scheme.

4   Discussion of Results

Series of computations was carried out for the influence of controlling thermo and hydrodynamic parameters on the dimensionless velocity(U), temperature(T) and concentration(C). The present analysis concerns the case of optically thick boundary layers where thermal boundary layer is expected to become very thick as the medium is highly absorbing. The Rosseland diffusion model adds radiative conductivity to the conventional thermal conductivity. The effect of radiation is to thicken the thermal boundary layer similar to the effect of decreasing Prandtl number. In this study, the default values for parameters are $Pr = 0.71$ (air), $Sc = 0.6, N = 3.0$, $M = 1.0$, $E_c = 0.001$, $Gr = 20, Gm = 20$, $D_a = 0.1$, $F_s = 0.1$, $Re = 1$. Unless otherwise stated on the graph, all the graphs correspond to these default values.

In order to validate the present scheme, we compared the present solutions with available solutions of Dada and Adefolaju [17] (see figure 2a and 2b). They employed the scheme to study the same flow field in the absence of Dufour and Soret. This comparison resulted in a good agreement.

Figure 3 shows the effect of N on the dimensionless velocity profile against Y-coordinate and it shows that an increase in N induces a rise in the steady state velocity profile. The increase gives a rapid rise in the velocity near the wall and the velocity decends smoothly towards zero.

Figure 4 shows the effect of Gr on the dimensionless velocity profile against Y-coordinate. From the graph, Gr indicates the relative effect of thermal buoyancy force to the viscous hydrodynamic force in the boundary layer. An increase in Gr induces a rise in the steady state velocity profiles, the increase gives a rapid rise in the velocity near the wall and the velocity descends smoothly towards zero.

Figure 5 depicts the effect of magnetic field M on the dimensionless velocity profile. Increase in the magnetic field causes reduction in the velocity profile. This is due to the fact that the application of magnetic field on an electrically conducting fluid results to a resistive type of force called *Lorentz force* which has tendency to slow down the motion of a fluid and its temperature.

Figure 6 illustrates the effect of conduction-radiation heat transfer parameter (N) on the temperature profile and it shows that an increase in N correspond to an increase in the contribution of conduction of thermal radiation heat transfer. As $N \to \infty$, conduction heat transfer dominates and the contribution of thermal radiative flush disappears. Small values of N corresponds physically to stronger thermal radiation flux and the maximum temperature are observed for $N = 0.5$. As N increases to 1.0, 2.0 and 5.0 considerable reduction is observed in the temperature values from the highest value at the wall ($Y = 0$) across the boundary layer to the free stream at which the temperature values are negligible for any value of N. All profiles decay to zero in the free stream.

The effect of Schmidt number (Sc) on the temperature profile is shown in figure 7. It is noticed that the temperature increases due to an increase in Sc. The figure shows that temperature increases rapidly with an increase in Sc, which correspond to an increase in chemical molecular diffusivity.

Figure 8 shows the effect of Dufour (Du) on dimensionless temperature profile. It is observed that an increase in Dufour brings about a decrease in the temperature.

Figure 9 shows the effect of Pr on the dimensionless temperature profile. Pr is the ratio of momentum diffusivity to thermal diffusivity i.e., it controls the thickness of the thermal boundary layer and the rate of heat transfer. The numerical results show that, as Prandtl number increases, a decrease in the thermal boundary layer thickness and in general lower average temperature is experienced. This is because smaller value of Pr increases the thermal conductivity of the fluid which indicates that heat is able to diffuse away from the heated surface more rapidly than higher values of Pr. Temperatures across the boundary layer normal to the wall reduces to zero faster for higher Pr values.

Figure 10 illustrates the effect of Soret (Sr) on the concentration profile. As Sr increases great increase in the concentration profile is experienced. The concentration decreases asymptotically to zero from the highest value at the wall to zero in the free stream.
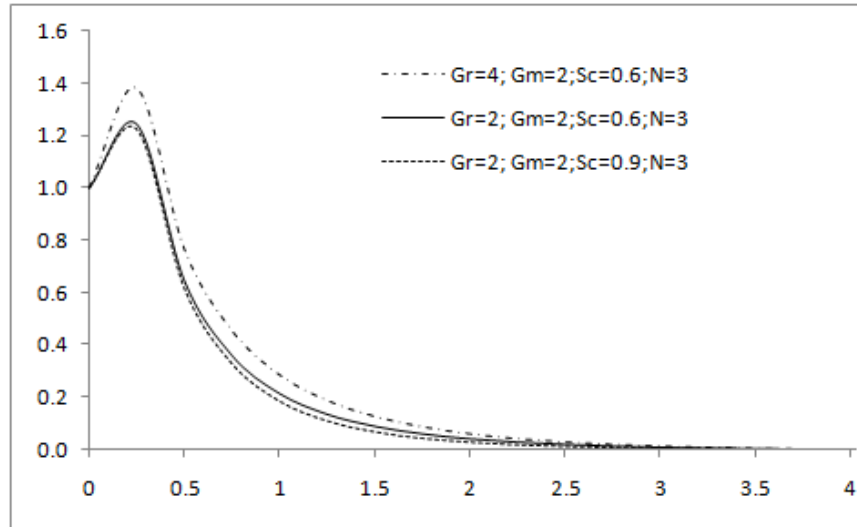
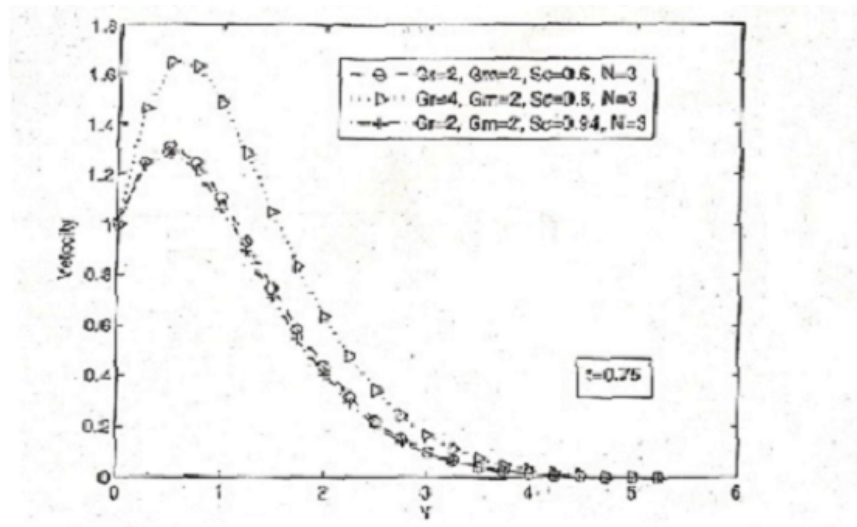Figure 2a: Velocity profile for various G_r, G_m, Sc and N(Present Result)

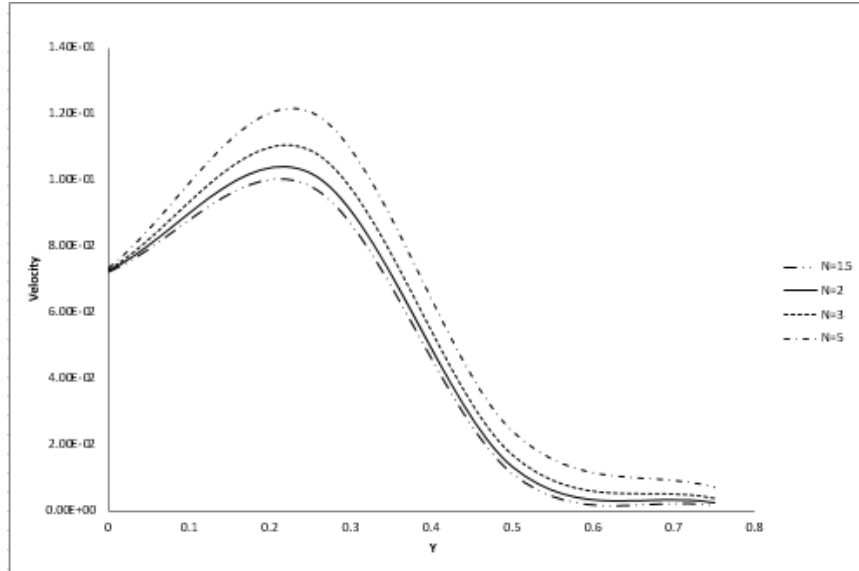Figure 2b: Velocity profile for various G_r, G_m, Sc and N(Dada and Adefolaju's Result)

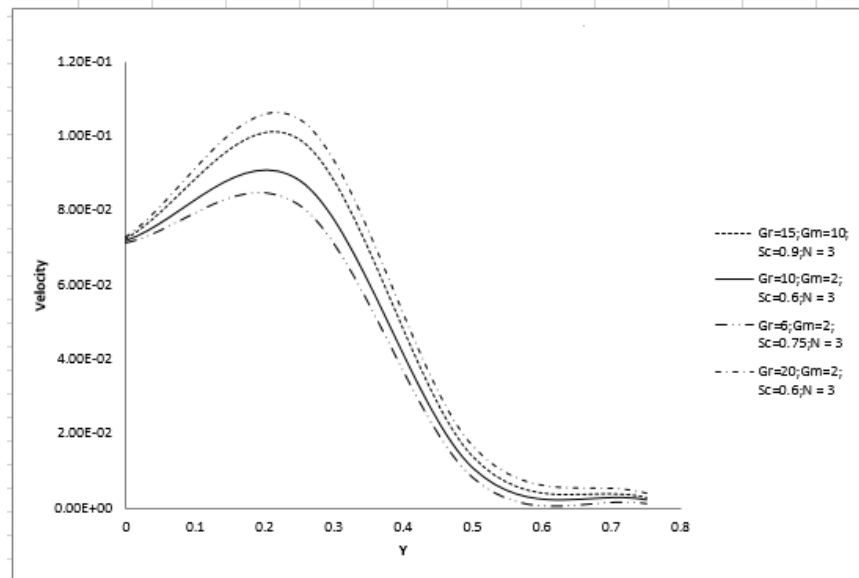Figure 3: Effects of Conductive Radiation Heat Transfer Parameter(N) on Temperature

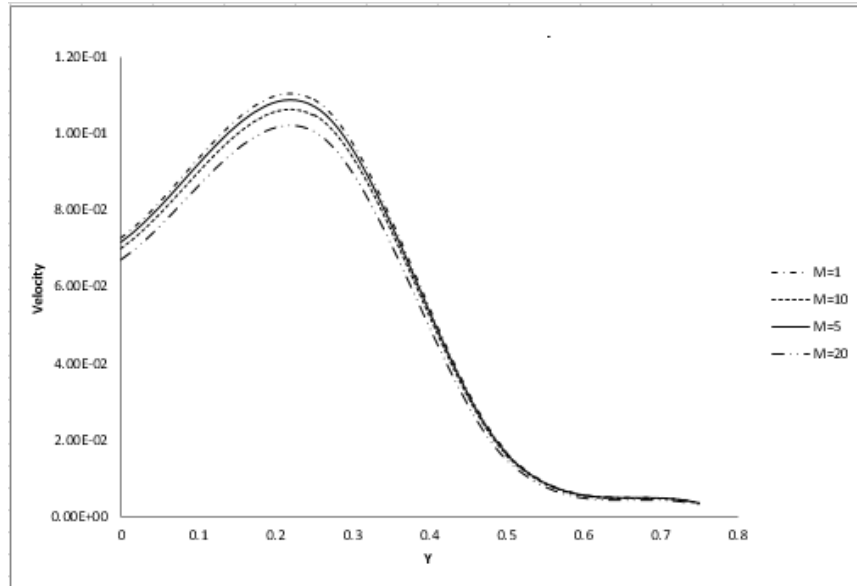Figure 4: Effects of G_r on Velocity Profile

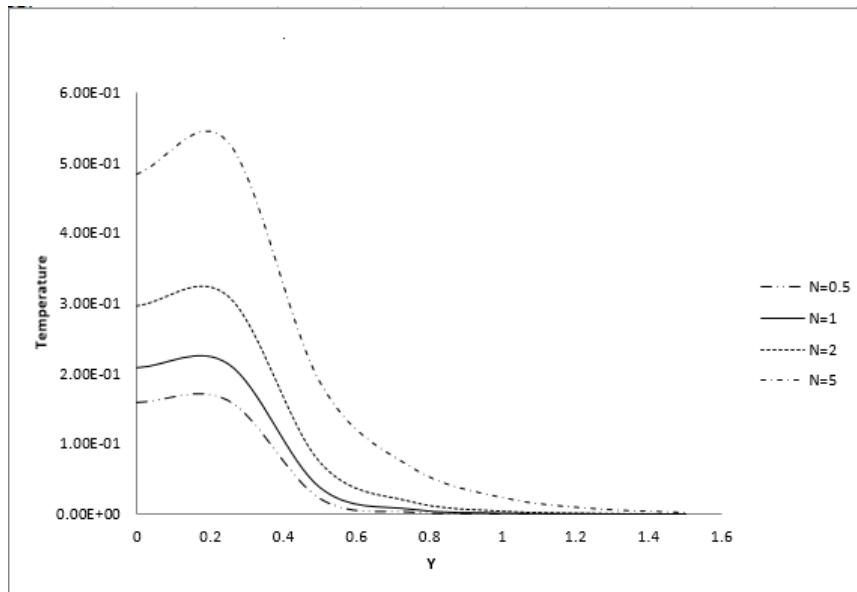Figure 5: Effects of Magnetic Field on Velocity Profile
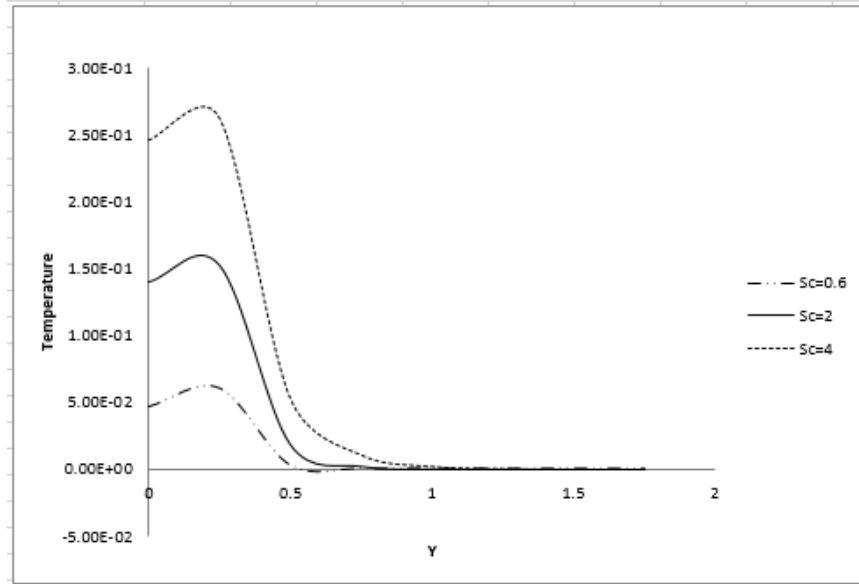

Figure 6: Effects of N on Velocity Profile
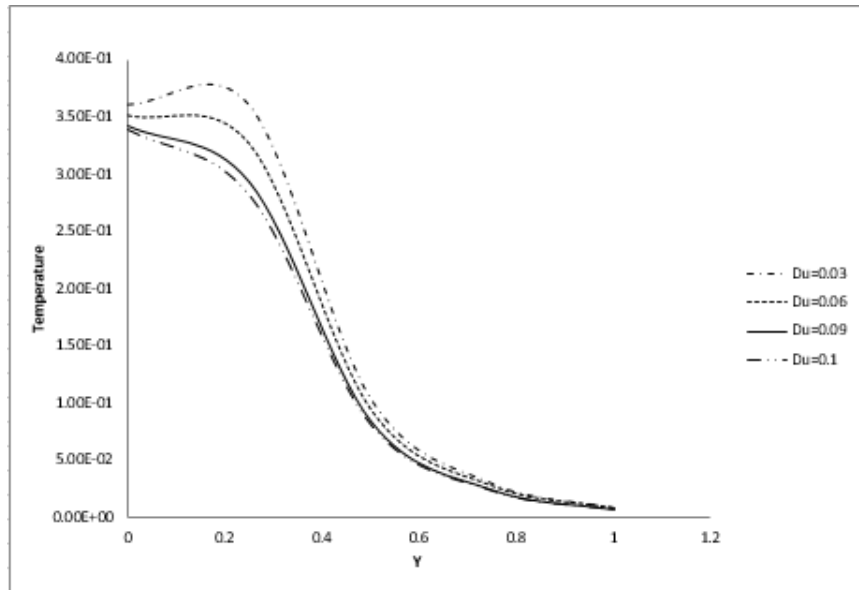
Figure 7: Effects of Sc on Temperature

Figure 8: Effects of Du on Temperature
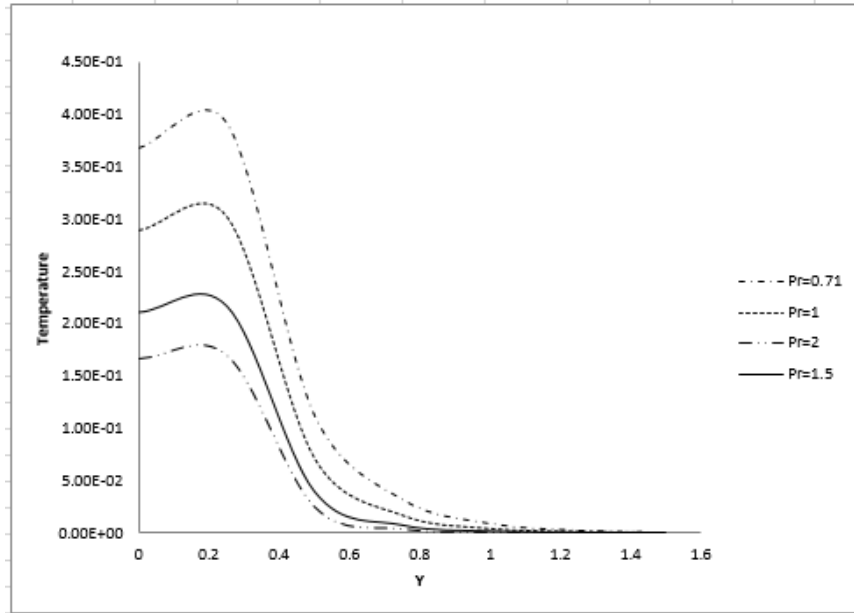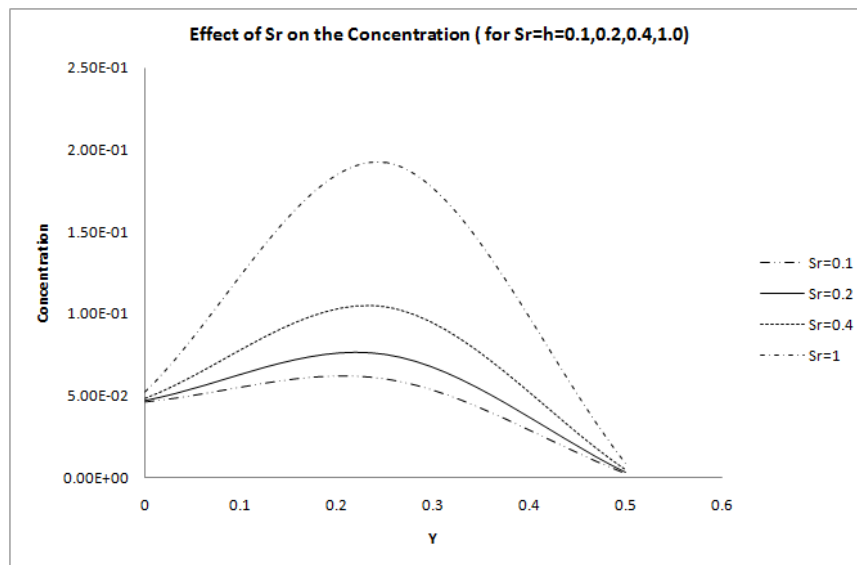
Figure 9: Effects of Pr on Temperature

Figure 10: Effects of Sr on Concentration

5   Conclusion

The study is concerned with the influence of controlling thermo fluid and hydrodynamics parameters (such as thermal Grashof number (Gr), solutal Grashof number (Gm), magnetic parameter (M), Darcy number (Da), etc) on the dimensionless velocity(U), temperature(T) and concentration(C) profiles of a viscous incompressible, gray, absorbing-emitting magnetohydrodynamics (MHD) fluid

flowing past an impulsively started vertical plate in a porous medium. The Rosseland diffusion flux model has been used to simulate the radiative heat flux. The family of governing partial differential equations is solved by an implicit finite difference scheme of Crank Nicolson type. A parametric study is perfrmed to illustrate the influence of thermo-physical parameters on the velocity, temperature and concentration profiles. Validation of the present results with the published results was carried out and good correlation was achieved.

Acknowledgement

References

[1] Loganatha, P., Iranian, D. and Ganesan, P. Effect of Chemical Reaction on Unsteady free Convective and Mass Transfer Flow Past a Vertical Plate with Variable Viscosity and Thermal Conductivity. *European Journal of Scientific Research* ISSN 1450-216X, vol. 59 issue 31, pp. 403-416, (2011).

[2] Alam, M.D., Ferdows, M., Ota, M. and Maleque, M.A. (2006). Dufour and Soret Effect of Steady Free Convection and Mass Transfer Flow Past a Semi-infinite Vertical Porous Plate in a Porous Medium. *Int. J. of Appl. Mech. and Engineering*, vol. 11, pp. 535-545, (2006).

[3] Mahajan, R.L., Gebhart, B.B. Viscous Dissipation Effects in Boundary-Induced Flows. *Int. J. of Heat and Mass Transfer*, vol. 7, pp. 26-45, (1989).

[4] Mansour, M.H. Radiative and free Convection Effects on the Oscillatory Flow Past a Vertical Plate.*Journal of Astrophysics Space Science*, vol. 166, pp. 26-45, (1990).

[5] Modest, M.F. Radiation Heat Transfer. McGraw-Hill, New York, (1993).

[6] Bratis, J.C., Novotny, J.R. Radiation-Convection Interaction in Boundary Layer Regime of an Enclosure, *Int. J. of Heat and Mass Transfer*, vol. 17, pp. 365-379, (1994).

[7] Chang, C. and Kang, K.T. Radiation Natural Convection interaction in two Dimensional Complex Enclosure, *ASME Journal of Heat Transfer*, vol. 105, pp. 89-95, (1983).

[8] Hossain, M.A., Kutibuddin, M. and Tarkar, H.S. Radiation Interaction on Combined Forced and Free Convection across a Horizontal Cylinder, *International Journal of Applied Mechanics and Engineering.* vol. 4, pp. 29, (1999).

[9] Chamkha, A.J. Aly, A.M. and Mansour, M.A. Natural Convective Power-Law Fluid Flow Past a Vertical Plate Embedded in a Non-darcian Porous Medium in the Presence of a Homogeneous Chemical Reaction. *Nonlienar Analysis, modeling and Control.* vol. 15, issue 2, pp. 139-154, (2010).

[10] Hall, M.G. The boundary Layer over an impulsively Started Flat Plate. *Proc. Ray. Soc.*, A, 310, 1502, pp. 401-414, (1969).

[11] Soundalgekar, V.M. and Takhar, H.S. Radiation Free Convective Flow of an Optically thin Gray Gas Past a Semi Infinite Vertical Plate. *Modeling Measurement and Control*, vol. B51, pp. 31-40, (1993).

[12] Muthuemaraswamy, R. Natural Convection of Flow Past on Impulsively Started Vertical Plate with Variable Surface Heat Flux. *Far East Journal of Applied Mathematics*, vol. 14, issue 1, pp. 99-109, (2004).

[13] Chamkha, A.J. Effect of Heat Absorption and Thermal radiation in Heat Transfer in a Fluid-Particle Flow Past a Surface in the presence of a Gravity Field. *Int. J. of Thermo sciences*. vol. 39, pp. 605-615, (2000).

[14] Mohammadein, A. A. and Mansour, M.A. Radiative Effects on Natural Convection Flows in a Porous Media. *Transport Porous Media*, vol. 32, issue 3, pp. 263-283, (1998).

[15] Takhar, H.S., Beg, O.A. and Kumari, M.A. Computational Analysis of Coupled Radiation Convection Dissipation Non-gray gas Flow in a Non-Darcy Porous Medium Using the Keller-Box Implicit Scheme. *Int. Journal of Energy Research*, vol. 22, pp. 141-159, (1998).

[16] Chamkha, A.J., Tarka, H.S., Soundalgekar, V.M. Radiation Effects on the Free Convective Flow Past a Semi-Infinite Vertical Plate with Mass Transfer, *Chemical Engineering Journal*, vol. 84, pp. 335-342, (2001).

[17] Dada M.S. and Adefolaju H.F. Dissipation, MHD and Radiation Effects on a steady convective Heat and Mass Transfer in a Darcy-Forcheimer Porous Medium. *Journal of Mathematics Research*, vol. 4, issue 2, pp. 110-127, (2012).

[18] Zeuco, J. Numerical Study of an Unsteady Free Convective Magnetohydrodynamics Flow of a Dissipative Fluid along a Vertical Plate Subject to Constant Heat Flux. *Int. J. of Engineering Science*, vol. 44, pp. 1380-1393, (2006).

[19] Idowu, A.S., Joseph, K.M., Onwubuoya, C., Joseph, W.D. Viscous Dissipation and Buoyancy effects on Laminar Convection in a Vertical Channel with Transpiration. *Center point Journal* (Science Edition) Vol. 21,issue 2, pp. 67-83, (2015).

[20] Berardi, P.G., Cuccurullu, G., Acierno, D. and Russo, P. Viscous Dissipation in Duct flow of Molten Polymers,*Proceedings of Eurotherm Semina*, vol. 46, pp. 39-43, (1995).

[21] Brewster, M.Q. Thermal radiactive transfer and properties. John Wiley and Sons, New York.(1992).

[22] Suneetha, S. and Bhaskar Reddy, N. Radiation and Darcy effects on Unsteady MHD Heat and Mass transfer flow of a Chemically Reacting Fluid past an impulsively started vertical plate with Heat Generation. *Int. J. of Appl. Math. and Mech.* vol. 7, issue 7, pp. 1-19, (2011).

[23] Carnahan, B., Luther, H.A. and Willkes, J.O. Applied Numerical Method, John Wiley and Sons, New York, (1969).

[24] Ramachandra Prasad V., Bhaskar Reddy N. and Muthucumaraswamy, R. Radiation and mass transfer effects on two-dimensional flow past an impulsively started isothermal vertical plate. *Int. Journal of Thermal Sciences*, vol. 46, issue 12, pp. 1251-1258, (2007).

[25] Ramachandra Prasad V. and Bhaskar Reddy N. Radiation and mass transfer effects on an unsteady MHD free convection flow past a heated particle plate in a porous medium with viscous dissipation. *Theoretical Applied Mechanics*, Vol. 34, issue 2, pp. 135-160, (2007).